Statistica Sinica Preprint No: SS-2019-0219	
Title	Nonparametric covariance estimation for mixed longitudinal studies, with applications in midlife women's health
Manuscript ID	SS-2019-0219
URL	http://www.stat.sinica.edu.tw/statistica/
DOI	10.5705/ss.202019.0219
Complete List of Authors	Anru Zhang and Kehui Chen
Corresponding Author	Anru Zhang
E-mail	anruzhang@stat.wisc.edu
Notice: Accepted version subject to English editing.	

Nonparametric covariance estimation for mixed longitudinal studies, with applications in midlife women's health

Anru R. Zhang[1,2] and Kehui Chen[3]

[1] *University of Wisconsin-Madison,* [2] *Duke University, and* [3] *University of Pittsburgh*

Abstract: Motivated by applications of mixed longitudinal studies, where a group of subjects entering the study at different ages (cross-sectional) are followed for successive years (longitudinal), we consider nonparametric covariance estimation with samples of noisy and partially-observed functional trajectories. The proposed algorithm is based on a sequential-aggregation scheme, which is non-iterative, with only basic matrix operations and closed-form solutions in each step. The good performance of the proposed method is supported by both theory and numerical experiments. We also apply the proposed procedure to a midlife women's working memory study based on the data from the Study of Women's Health Across the Nation (SWAN).

Key words and phrases: longitudinal studies, cross-sectional, partial trajectories, functional data, covariance estimation, consistency.

1. Introduction

A mixed longitudinal study is a mixture of a longitudinal study and a cross-sectional one (Berger, 1986; Helms, 1992). Suppose the researchers intend to study the social and cognitive development of children aged 4 - 12. In an ideal longitudinal design, a group of 4-year-old children will be recruited and followed during 8 successive years. Alternatively, in a mixed longitudinal design, one may recruit a group of children aged between 4 - 8 and follow them for 4 years (within a typical funding period). Since the age requirement is more flexible at recruitment, this type of mixed longitudinal design results in shorter completion time and potentially larger group size. However, this type of mixed longitudinal design also brings new challenges for statistical analysis, because the trajectory is only partially observed for each subject.

Specifically, we consider the data example from the Study of Women's Health Across the Nation (SWAN). SWAN is a community-based, longitudinal study of midlife women. Women aged between 42 to 52 years were enrolled around 1996/97 and followed annually thereafter. Currently, SWAN data up to the 10th follow up visit are available in a publicly accessible repository managed by ICPSR, at `http://www.icpsr.umich.edu/icpsrweb/ICPSR/series/00253`. Although there were many other studies

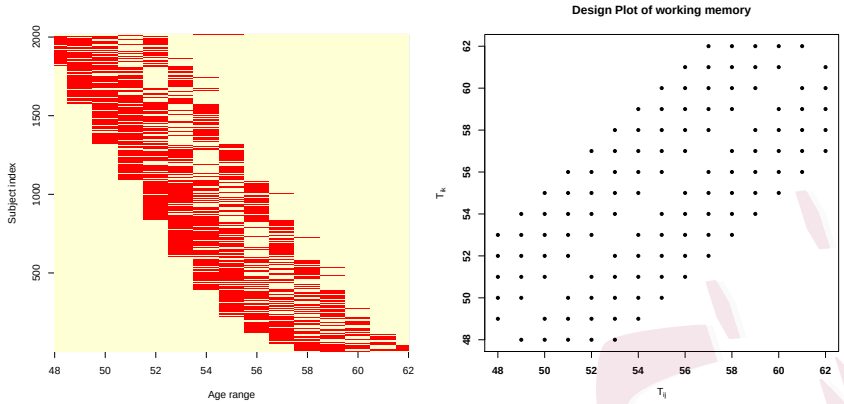

Figure 1: Left: For each of the 2016 subjects, measurements were between age x to $x+5$ for some $x \in [48, 58]$. Right: The design plots for covariance $G(s,t)$, i.e, the assembled pairs of (t_{ij}, t_{il}) for $1 \le i \le n, 1 \le j < l \le n_i$. The pooled pairs do not fill the entire domain $\mathcal{T}^2$ since there are no measurements available for any pairs of (t_{ij}, t_{il}) whenever $|j-l| > 5$.

of cognitive functioning in midlife, there are few longitudinal ones, and most of them were based on three or fewer cognition assessments (Karlamangla et al., 2017). Thus the study of within-person longitudinal declines in cognitive performance in those under 60 years of age is underdeveloped (Hedden and Gabrieli, 2004; Rönnlund et al., 2005). In contrast, the SWAN data contain more follow-ups and a wider age range, which provide a nice opportunity for a longer-term study of women's midlife health. Particularly, we focus on working memory measurements available from Visits 6 - 10. By

pooling all subjects together, the age range under consideration is a span of 15 years: $\mathcal{T} = [48, 62]$. However, with a mixed longitudinal design, the longitudinal follow-ups of each subject in SWAN only capture a small piece of the chronological aging trajectory, and the shape might have complex interaction with age (Rönnlund et al., 2005; Fuh et al., 2006); as we can see from the left panel of Figure 1, the measurements for each subject are only a subset within a period of at most 5 years. Traditional parametric models such as LMM (with age as a between-subject effect, and the time of follow-ups as a within-subject effect) often assume a linear trend over time, but the individual chronological aging trajectories of working memory might have a complex shape. For example, the working memory might improve first and then decline, and the age that the working memory starts to decline varies among subjects. Therefore, we believe that nonparametric modelings such as functional principal component analysis may reveal interesting features.

We particularly consider a mixed longitudinal design for n subjects, where for each subject k, measurements are obtained at times t_{kj} for $k = 1, \ldots, n$ and $j = 1, \ldots, n_k$. We use the notation

$$X_k(t_{kj}) = Z_k(t_{kj}) + \epsilon_{kj}, \quad t_{kj} \in \mathcal{T}, \tag{1.1}$$

where ϵ_{kj} are zero mean i.i.d. measurement errors that are uncorrelated

with all other random components and satisfy $\text{var}(\epsilon_{kj}) = \sigma^2$. $Z(t), t \in \mathcal{T}$ is assumed to be a square-integrable random process with mean and covariance functions $\mu(t)$ and $G(s,t) = \text{Cov}(Z(s), Z(t))$. In a mixed longitudinal design, the observed time points $\{t_{kj}\}_{j=1,\ldots,n_k}$ for each subject k are restricted to a subject-specific partial domain. As shown in the right panel of Figure 1, we do not have the within-subject correlation information for any two points that are more than 5 years apart in the SWAN data example. To apply a functional data approach for mixed longitudinal studies, the main methodological challenge is to non-parametrically estimate the covariance structure G of the underlying process.

The estimation of the mean and covariance functions plays fundamentally important roles in functional data analysis. Useful tools such as functional principal component analysis often rely on a consistent covariance function estimation (Yao et al., 2005; Hall and Hosseini-Nasab, 2006; Li and Hsing, 2010). For conventional functional data, where the pooled design (right panel of Figure 1) for covariance is complete, various methods based on kernel smoothing and splines have been proposed (e.g., Rice and Silverman (1991); Yao et al. (2005); Peng and Paul (2009); Xiao et al. (2013)). In some previous studies where the covariance information is incomplete, Fan et al. (2007) considered a semi-parametric covariance estimation where

the variance function $G(t,t) = \sigma^2(t)$ is modeled non-parametrically under smoothness conditions, while the off-diagonal correlation structures are assumed to have a parametric form $\rho(s,t,\theta)$. We would like to mention that this problem is different from the banded covariance estimation considered in previous literature such as Bickel and Levina (2008); Cai et al. (2010); Cai and Yuan (2012); Cai et al. (2016) and the references therein since there is no bandable covariance structure in our scenario, though the design pairs are only within a banded area.

We propose to estimate the covariance via a sequential-aggregation scheme (detailed in Section 2). The proposed algorithm is non-iterative, with closed-form solutions and only basic matrix operations (such as matrix multiplication and singular value decomposition) in each step. We prove that under moderate conditions as specified in Section 3, the proposed method can consistently recover the nonparametric covariance structure based on data within a banded area. One key step of the proposed procedure is solving the orthogonal Procrustes's or Wahba's problem (Wahba, 1965), i.e. finding a rotation matrix to best align two sets of points in two different Euclidean coordinate systems. This problem was first motivated by satellite attitude determination, then later applied to many other applications. To theoretically analyze the procedure, we introduce a new error

bound for the solution to Wahba's problem (Lemma 1). In the theoretical analysis, we also introduced a series of technical tools on perturbation inequalities of singular subspaces, including Lemmas 3, 5, 7, and 8, which may be of independent interest.

The analysis of fragmentary functional observations have been studied under other modeling assumptions, for example Delaigle and Hall (2013) and Delaigle and Hall (2016). Very recently, two manuscripts Descary and Panaretos (2018) and Kneip and Liebl (2017) considered covariance estimation and reconstruction from fragmentary functional observations using an optimization framework. The implementations of both works involve iterations. In particular, Descary and Panaretos (2018) formulates the problem as a non-convex optimization, which aims to minimize the error within the observable diagonal band under rank constraint. Distinct from the previous approaches in the literature, in this paper, we introduce a novel sequential-aggregation approach that provides more explicit solutions and new insights into the covariance estimation problem. We also include numerical comparisons with their method in the simulation section. In addition, this problem is also related to several recent works on high-dimensional covariance estimation with missing values. For example, Loh and Wainwright (2012); Lounici et al. (2014) considered the linear regression or covariance matrix

estimation where the observations are missing randomly with a fixed rate, while Kolar and Xing (2012); Cai and Zhang (2016) considered a more general setting that allows a non-random missing pattern, but still requires that each pair of covariates simultaneously appear in a sufficient number of samples. The problem discussed in this paper is distinct from these existing settings since a large portion of covariate pairs will never appear in the same sample (such as the pairs between the earlier and latest observations in the longitudinal studies) by the nature of the design. Bishop and Byron (2014) has studied a similar sequential-aggregation scheme for matrix completion, however, they mainly consider the completion of high-dimensional low rank positive semidefinite matrix in a deterministic setting, while we provide a statistical guarantee for covariance estimation from partially-observed noisy functional data.

The rest of this article is organized as follows. The methodology and algorithm are described in Section 2, followed by theoretical analyses in Section 3. In Section 4, we present a series of numerical experiments, including the application to SWAN data. The proofs are collected in the supplementary materials.

2. Covariance Estimation for Mixed Longitudinal Design

We briefly introduce the notation that will be used throughout the paper. For a matrix $A \in \mathbb{R}^{p_1 \times p_2}$ or bivariate function G, let $\{\sigma_1(A), \sigma_2(A), \ldots\}$ and $\{\sigma_1(G), \sigma_2(G), \ldots\}$ be the singular values in non-increasing order. We adapt the R syntax to indicate matrices/functions restricted to the subsets of indices/domains: if $A \in \mathbb{R}^{p_1 \times p_2}$, $a \leq b, c \leq d$ are four positive integers, we use $A_{[a:b,c:d]}$ to denote the submatrix of A formed by its a-th to b-th rows and c-th to d-th columns; ":" alone represents the entire index set, so $A_{[:,1:r]}$ and $A_{[a:b,:]}$ represent the first r columns of A and the $\{a, \ldots, b\}$-th rows of A, respectively; similarly $G_{[\mathcal{T}_1,\mathcal{T}_2]}$ represents function G with domain $\mathcal{T}_1 \times \mathcal{T}_2$. Let $\mathcal{L}(\mathcal{T})$ be the Lebesgue measure of any domain $\mathcal{T}$. Let $\|A\|_F$ and $\|A\|$ be the matrix Frobenius norm and operator norms, respectively: $\|A\|_F = \left(\sum_{i,j} A_{ij}^2\right)^{1/2} = \left(\sum_i \sigma_i^2(A)\right)^{1/2}$, $\|A\| = \sigma_{\max}(A)$. Denote $I_{r\times r}$ as the r-by-r identity matrix and $\mathbb{O}_{p,r} = \{V : V^\top V = I_{r\times r}\}$ as the set of all p-by-r matrices with orthonormal columns. In particular, the set of all r-by-r orthogonal matrices can be denoted as $\mathbb{O}_r = \mathbb{O}_{r,r}$. Denote $\|G\|_{HS} = \left(\iint |G(s_1, s_2)|^2 ds_1 s_2\right)^{1/2}$ as the Hilbert-Schmidt norm of the bivariate function G. Finally, we use $C, C_0, C_1, c, c_0, \ldots$ to represent generic constants, whose exact values may vary from line to line.

Suppose $\mathcal{T}$ is the entire period of interest. Consider an equally spaced

grid of time points $T = \{t_1, \ldots, t_p\}$ on the time domain $\mathcal{T}$. In a mixed-longitudinal design, suppose $\mathcal{T}_k$ is the observational period for subject k and we observe $X_k(T_k)$ in the contiguous band of the domain $\mathcal{T}_k$:

$$\mathcal{T}_k \subseteq \mathcal{T}, \quad \frac{\mathcal{L}(\mathcal{T}_k)}{\mathcal{L}(\mathcal{T})} = \delta, \quad T_k \subseteq T \cap \mathcal{T}_k = \{t_1, \ldots, t_p\} \cap \mathcal{T}_k, \quad k = 1, \ldots, n.$$

Here, the fraction of observation δ is assumed to be a constant between 0 and 1 and T_k might not be consecutive due to missing values. If T_k is complete with no missing values, the number of observations is d with $\delta = d/p$. Suppose the signal-noise decomposition (1.1) holds for each observation: $X_k(t_{kj}) = Z_k(t_{kj}) + \epsilon_{kj}$. Let Σ_0 denote the $p \times p$ discretized version of covariance G, i.e., the (i, j)-th entry of Σ_0 equals $\mathrm{Cov}(Z(t_i), Z(t_j)) = G(t_i, t_j)$. We fulfill the estimation of G via the discretized version Σ_0. Suppose G has approximate rank r. Then, we will also have $\Sigma_0 \approx AA^\top$, where $A \in \mathbb{R}^{p \times r}$ can be regarded as the factors of Σ_0.

We consider a sequential-aggregation-based algorithm. We first divide $\mathcal{T}$ into a series of overlapping sub-domains, then obtain estimates of A on each sub-domain. Next, we aggregate all estimates on sub-intervals into a full estimate of A. Here, a crucial rotation operation is involved in the aggregation step to ensure that the estimates of A on each sub-domain are aligned. Finally, one can obtain an estimate of Σ_0 from $\tilde{A}\tilde{A}^\top$, where $\tilde{A}$ is an estimate of A up to a rotation. Then G is recovered by a standard

interpolation technique. The detailed steps are described as follows and illustrated in Figure 2. For any sub-index set $I \subseteq \{1, \ldots, p\}$, we use the notation $T(I) = \{t_i : i \in I\}$ and $(X_k)_I = X_k(T(I))$.

Step 1 For a chosen band parameter b and an increment parameter a satisfying $1 \leq a \leq b - r \leq b \leq d$, we construct the following sub-index set:

$$I_l = \{(l-1)a + 1, \ldots, \{(l-1)a + b\} \wedge p\}, \quad l = 1, \ldots, l_{\max}. \tag{2.2}$$

Here $l_{\max} = 1 + \lceil (p-b)/a \rceil$ is the total number of sub-index sets. Each of I_l except the last one contains b indices and the last one contains at most b indices.

Step 2 For $l = 1, \ldots, l_{\max}$, we search for all samples that have full observations in I_l and denote the set of such samples as J_l:

$$J_l = \{1 \leq k \leq n : T(I_l) \subseteq T_k\}.$$

Then the sample covariance matrix for indices in I_l is calculated as

$$\begin{aligned} &\hat{\Sigma}_l \in \mathbb{R}^{|I_l| \times |I_l|}, \quad \hat{\Sigma}_l = \frac{1}{n_l^*} \sum_{k \in J_l} \left((X_k)_{I_l} - \bar{X}_{I_l}\right) \left((X_k)_{I_l} - \bar{X}_{I_l}\right)^\top, \\ &n_l^* = |J_l|, \quad \bar{X}_{I_l} = \frac{1}{n_l^*} \sum_{k \in J_l} (X_k)_{I_l}. \end{aligned} \tag{2.3}$$

Step 2' Alternative to only using the subjects that have full observations in I_l, we can also implement the option that using all the data available for

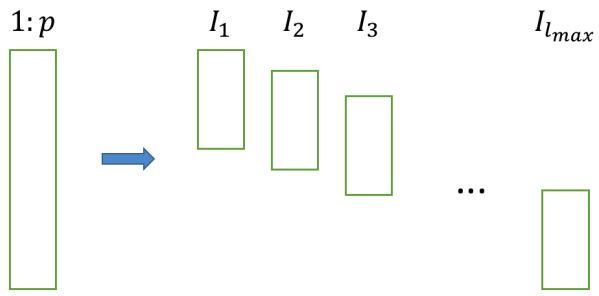

(a) Step 1. Construction of I_l, $l = 1, \ldots, l_{\max}$

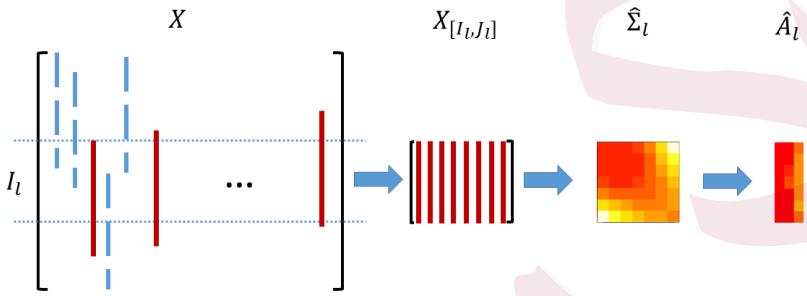

(b) Step 2-3. Construction of $\hat{\Sigma}_l$ and $\hat{A}_l$, $l = 1, \ldots, l_{\max}$

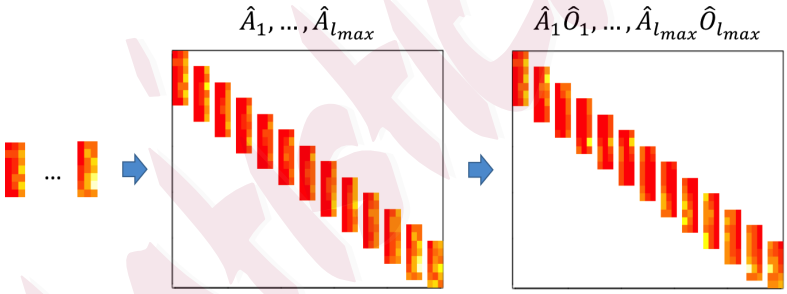

(c) Step 4. Rotate $\hat{A}_l$ via $\hat{O}_l$

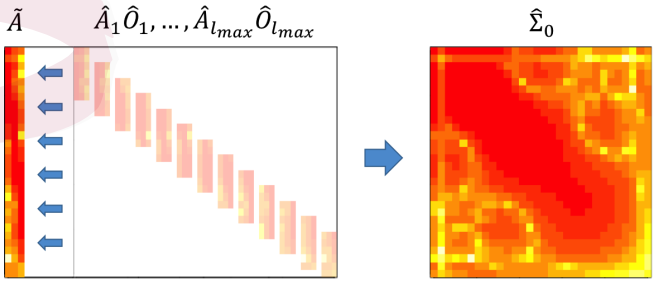

(d) Steps 5 and 6. Aggregate $\hat{A}_l$ to $\tilde{A}$ and calculate $\hat{\Sigma}_0 = \tilde{A}\tilde{A}^\top$

Figure 2: Illustration of the procedure

the pair $(I_l(i), I_l(j))$ when computing $\hat{\Sigma}_{l,[ij]}$. This scheme is preferred to Step 2 when large portions of subjects have missing values, i.e., $X_k(T_k)$ are not complete consecutive observations (see Theorem 1 and Remark 4 for more discussions): $\hat{\Sigma}_l \in \mathbb{R}^{|I_l|\times|I_l|}, \bar{X}_{I_l} \in \mathbb{R}^{|I_l|}$,

$$\hat{\Sigma}_{l,[ij]} = \frac{\sum_{k:T(I_l(i)),T(I_l(j))\in T_k} \left((X_k)_{I_l(i)} - \bar{X}_{I_l(i)}\right)\left((X_k)_{I_l(j)} - \bar{X}_{I_l(j)}\right)}{(n^*)_{i,j,l}},$$

$$n^*_{i,j,l} = \left|\{k : T(I_l(i)), T(I_l(j)) \in T_k\}\right|,$$

$$\bar{X}_{I_l(i)} = \frac{\sum_{k:T(I_l(i)),T(I_l(j))\in T_k}(X_k)_{I_l(i)}}{n^*_{i,l}}, \quad n^*_{i,l} = \left|\{k : T(I_l(i)) \in T_k\}\right|. \tag{2.4}$$

Step 3 Evaluate the eigenvalue decomposition and the rank-r truncation of $\hat{\Sigma}_l$ as

$$\hat{\Sigma}_l = \hat{U}_l\hat{D}_l\hat{U}_l^\top, \quad \hat{\Sigma}_l^{(r)} = \hat{U}_{l,[:,1:r]}\hat{D}_{l,[1:r,1:r]}\hat{U}_{l,[:,1:r]}^\top. \tag{2.5}$$

Then for $l = 1, \ldots, l_{\max}$, we evaluate $\hat{\sigma}_l^2 = (\frac{1}{|I_l|-r}\sum_{i=r+1}^{|I_l|}\hat{D}_{l,[i,i]}) \vee 0$ as the sample variance of the noise and

$$\hat{A}_l = U_{l,[:,1:r]}\left\{(D_{l,[1:r,1:r]} - \hat{\sigma}_l^2 \cdot I_{r\times r}) \vee 0\right\}^{1/2} \in \mathbb{R}^{|I_l|\times r} \tag{2.6}$$

as the estimate of A on the sub-domain I_l. Here $I_{r\times r}$ is the r-by-r identity matrix. By these calculations, we expect that $\hat{A}_l\hat{A}_l^\top \approx \Sigma_{0,l} = (\Sigma_0)_{[I_l,I_l]}$.

Step 4 We construct a suitable right rotation on $\hat{A}_l$ so that all the pieces can be aligned. Specifically, we first let $\hat{O}_1 = I_{r\times r}$, then calculate $\hat{O}_{l+1}$

sequentially as

$$\hat{O}_{l+1} = \underset{O \in \mathbb{O}_r}{\arg\min} \left\| (\hat{A}_l)_{[(a+1):b,:]} \hat{O}_l - (\hat{A}_{l+1})_{[1:(b-a),:]} O \right\|_F^2, l = 1, \ldots, l_{\max} - 1. \tag{2.7}$$

Here, the row indices of $(\hat{A}_l)_{[(a+1):b,:]}$ and $(\hat{A}_{l+1})_{[1:(b-a),:]}$ both correspond to $[la+1, (l-1)a+b] \subseteq \{1, \ldots, p\}$. (2.7) is actually the orthogonal Procrustes's or Wahba's problem (Wahba, 1965), which can be solved by

$$\hat{O}_{l+1} = \tilde{U}\tilde{V}^\top, \text{ where } \tilde{U}\tilde{\Sigma}\tilde{V}^\top = (\hat{A}_{l+1})^\top_{[1:(b-a),:]} (\hat{A}_l)_{[(a+1):b,:]} \hat{O}_l \text{ is the SVD.} \tag{2.8}$$

Step 5 In this step, we aggregate all pieces $\hat{A}_l \hat{O}_l$ into one complete factor $\tilde{A} \in \mathbb{R}^{p \times r}$. For convenience of notation, we "frame" the $|I_l|$-by-r matrix $\hat{A}_l$ to its original p-by-r factor scale, $\hat{A}^*_l \in \mathbb{R}^{p \times r}$, $\hat{A}^*_{l,[I_l,:]} = \hat{A}_l \hat{O}_l$, and $\hat{A}^*_{l,[I_l^c,:]} = 0$. For $1 \le i \le p$ and $1 \le j \le r$, we calculate

$$\tilde{A}_{[i,j]} = \frac{\sum_{l:i \in I_l} \hat{A}^*_{l,[i,j]}}{|\{l : i \in I_l\}|}. \tag{2.9}$$

Step 6 After the sequential aggregation, we finally estimate Σ_0 by

$$\hat{\Sigma}_0 = \tilde{A}\tilde{A}^\top \in \mathbb{R}^{p \times p}, \tag{2.10}$$

then linear interpolate between grid points to obtain $\hat{G}$ (Press et al., 1992, Chapter 3.6). Some smoothing instead of linear interpolation

might be useful in data applications for smoother results and better visualization.

Computation and Tuning Parameters: In summary, the proposed algorithm is non-iterative with only basic matrix calculations such as matrix multiplications and SVD, which can be implemented efficiently. The algorithm need the input of a, b, and the rank r. According to our simulation studies in Section 4, the performance of the method is not very sensitive to the selection of a and b. In numerical implementation, we suggest to select b to be slightly smaller than bandwidth d and select a to be a small increment (in practice $a = 0.1 \times d$ usually provides good enough result). In the following, we describe the random sub-sampling cross-validation method (Picard and Cook, 1984) to select the rank r.

We first randomly split n observations $\{X_k(T_k)\}_{k=1}^n$ into the training and testing groups of sizes $n_1 \approx \frac{(K-1)n}{K}$ and $n_2 \approx \frac{n}{K}$ for T times. For the t-th split, let $J_{\text{train}}^{(t)}$ and $J_{\text{test}}^{(t)}$ be the index sets for training and testing groups, respectively. For each $r \in \{1, \ldots, b-a\}$, we apply the proposed procedure on the training dataset $\{X_k(T_k)\}_{k \in J_{\text{train}}^{(t)}}$ and denote the outcome as $\hat{\Sigma}^{(t)}(r)$. Then we calculate the sample covariance matrix $\hat{\Sigma}_{\text{test}}^{(t)} \in \mathbb{R}^{p \times p}$ based on the

samples from the testing group,

$$(\hat{\Sigma}^{(t)}_{\text{test}})_{[i,j]} =$$

$$\begin{cases} \sum_{\substack{k\in J^{(t)}_{\text{test}} \\ T_k\ni T(i),T(j)}} (X_{ik}-\bar{X}_i)(X_{jk}-\bar{X}_j) \Big/ \sum_{\substack{k\in J^{(t)}_{\text{test}} \\ T_k\ni T(i),T(j)}} 1, & \text{if } \sum_{\substack{k\in J^{(t)}_{\text{test}} \\ T_k\ni T(i),T(j)}} 1 \geq n_0, \\ \text{NA}, & \text{otherwise,} \end{cases}$$

where n_0 is the lower threshold in evaluating testing sample covariance matrix. Then we evaluate the prediction error as

$$E(r) = \sum_{t=1}^{T} \sum_{(\hat{\Sigma}^{(t)}_{\text{test}})_{[i,j]}\neq \text{NA}} \left((\hat{\Sigma}^{(t)}(r))_{[i,j]} - (\hat{\Sigma}_{\text{test}})_{[i,j]} \right)^2.$$

Here to improve accuracy, we only evaluate the prediction errors on those (i, j) pairs where $(\hat{\Sigma}_{\text{test}})_{[i,j]}$ is evaluated based on at least n_0 samples. Finally, we choose $\hat{r} = \arg\min_{1\leq r\leq b-a} E(r)$ and apply the proposed procedure with $\hat{r}$ to obtain the final estimator $\hat{\Sigma}_0$. In our simulations, we used $K = 5$, $T = 10$ and $n_0 = 4$, and other cross-validation methods are expected to yield similar results.

In practice, we propose to use the cross-validation method because this usually prevents under-selection. We observed a slight over-selection of r in simulations, but over-selection is not a problem for covariance estimation as the components (eigenvalues) beyond r are all assumed to be very small. The numerical performance of the proposed procedure based on cross-validation and the effect of tuning parameters will be further investi-

gated in Section 4.

3. Theoretical Analysis

Before presenting the main theoretical results, we first introduce the following assumptions.

Assumption 1. There is a positive integer r such that the eigenvalues of G satisfy $\lambda_1(G) \geq \cdots \geq \lambda_r(G) > \lambda_{r+1}(G) \geq \cdots \geq 0$. Let $G^{(r)}$ be the best rank-r approximation for G and $G^{-(r)} = G - G^{(r)}$. We also assume $\|G\|_{HS} < \infty$, $\|G^{(-r)}\|_{HS} \leq \frac{C}{\sqrt{n^*}}$, where n^* is the effective sample size defined later in Theorem 1.

The rank r is allowed to increase slowly as n and p grow. The (approximate) reduced rank covariance structure has been explored by James et al. (2000) and Peng and Paul (2009) for sparse functional data, where only a few irregularly (randomly) spaced observations are available on each subject. They view the rank restriction as a form of regularization to avoid over-parametrization. The same reasoning applies to our scenario, as only a fraction of trajectories are observed for each subject.

Assumption 2. For any contiguous subdomain $\tilde{\mathcal{T}} \subseteq \mathcal{T}$, we define $G^{(r)}_{[\tilde{\mathcal{T}},\tilde{\mathcal{T}}]} = G^{(r)}(s,t)_{s\in\tilde{\mathcal{T}},t\in\tilde{\mathcal{T}}}$. There exists a constant $0 < \kappa < \delta$ such that

$\gamma = \max_{\frac{\mathcal{L}(\tilde{\mathcal{T}})}{\mathcal{L}(\mathcal{T})} \geq \kappa} \{\mathrm{tr}(G) \frac{\mathcal{L}(\tilde{\mathcal{T}})}{\mathcal{L}(\mathcal{T})} / \lambda_r \left(G^{(r)}_{[\tilde{\mathcal{T}}, \tilde{\mathcal{T}}]} \right)\}$ satisfies $\gamma = o((n^*)^{1/2})$.

Intuitively speaking, this assumption imposes a lower bound of C/γ on the r-th eigenvalues of $G_{[\tilde{\mathcal{T}}, \tilde{\mathcal{T}}]}$. It essentially ensures that G restricted on different contiguous subdomain $[\tilde{\mathcal{T}}, \tilde{\mathcal{T}}]$ is non-singular, so that the estimation of G only through segments of functional observations is possible. For a counter-example, if G have two "spikes" in the sense that only $G_{[0:0.2,0:0.2]}$ and $G_{[0.8:1,0.8:1]}$ have significant amplitudes, while $G_{[0.2:0.8,0.2:0.8]}$ is zero. Then the estimation of the cross-covariance parts $G_{[0:0.2,0.8:1]}$ and $G_{[0.8:1,0:0.2]}$ is impossible when one can only observe functional segments of length no more than 0.6. In addition, γ is allowed to increase moderately as n and p grow. Note that $\gamma \geq r$ and in the scenarios that γ/r is big, the method using complete observations only (step 2) is better than step 2'.

Assumption 3. Assume X satisfies moment condition $\sup_t \mathbb{E}|X(t)|^4 \leq C$.

Assumption 4. There exists $L > 0$ such that $|G(s,t) - G(s',t')| \leq L \max(|s - s'|, |t - t'|)$, $\forall\ s, s', t, t' \in \mathcal{T}$.

Since we used sample covariance approach and interpolate between observed grid points, Lipschitz condition is almost necessary. It is easy to satisfy as we work with a finite domain $\mathcal{T}$, and is weaker than second differentiable conditions usually used in smoothing methods.

We can now state the main results of this paper.

Theorem 1. Suppose Assumptions 1-4 hold. We take $b = \beta p, a = \alpha p$ for some constants $0 < \alpha < \beta \leq \delta < 1$. Assume $\beta - \alpha \geq \kappa \geq 2r/p$ (κ and r were defined in the assumptions), $n \geq Cp$, $p \geq C\gamma$, then the proposed procedure yields

$$\mathbb{E}\|\hat{G} - G\|_{HS} = O\left(\sqrt{\gamma^2/n^*} + p^{-1}\right). \tag{3.11}$$

Here, $n^* = \min_l n_l^*$ and n_l^* is defined in (2.3), if we use complete samples to calculate $\hat{\Sigma}_l$ via (2.3) of Step 2; $n^* = \min_{i,j,l} n_{i,j,l}^*$ and $n_{i,j,l}^*$ is defined in (2.4), if we use both complete and incomplete samples to calculate $\hat{\Sigma}_l$ by (2.4) of Step 2'.

Remark 1. The first error term in (3.11) is due to estimating errors of the discretized covariance Σ_0. The second error term p^{-1} is from the linear interpolation of the discretized Σ_0.

Remark 2. Theorem 1 provides theoretical guarantees for the proposed procedure under general mixed longitudinal designs (conditional on T_k), where the effective sample size, i.e., n^*, is driven by the minimum number of samples that cover each sub-interval I_l. In a balanced design where $T_k \subseteq T(\{w_k, \ldots, w_k + d - 1\})$ with w_k evenly chosen from $\{1, \ldots, p - d + 1\}$

for $k = 1, \ldots, n$, the boundary sub-intervals I_1 and $I_{l_{\max}}$ will have less effective sample size than the middle ones, which will yield a higher estimation error for the boundary part of G. To overcome such the bottleneck, we recommend a boundary-enriched design: beyond the balanced design as mentioned above, we include $n_a = cn$ additional ones with $T_k = T(\{1, \ldots, d\})$ or $T(\{p - d + 1, \ldots, p\})$ for a small constant $0 \leq c \leq 1$. Alternatively, one can apply an extended-domain design: for each $k = 1, \ldots, n$, $T_k = T(\{w_k, \ldots, w_k + d - 1\}) \cup T(\{1, \ldots, p\})$ with w_k uniformly chosen from $\{(2 - d), \ldots, p\}$. Under both the boundary-enriched and extended-domain designs, the result of Theorem 1 yields (3.11).

Remark 3 (Proof sketch of Theorem 1)**.** After introducing a series of notation, we develop error bounds for $\hat{A}_l$ (the outcome of Step 3), $\hat{O}_l$ (the outcome of Step 4), $\tilde{A}$ (the outcome of Step 5), then $\hat{\Sigma}_0$ and the final estimator $\hat{G}$ (the outcome of Step 6). In particular, Step 4 of the proposed procedure involves solving the orthogonal Procrustes problem (or Wahba's problem) (2.7). To derive the error bound of $\hat{O}_l$ from the error bound of $\hat{A}_l$, we introduce the following key Lemma 1 that provides a theoretical guarantee for the solution of (2.7). In addition, Lemma 1 is stronger than the previous results (c. f., (Bishop and Byron, 2014, Lemma 16)), which may be of independent interest.

Lemma 1 (Perturbation bound for Wahba's problem)**.** Suppose $A_1, A_2, A \in \mathbb{R}^{m\times r}$, $O_1, O_2 \in \mathbb{O}_r$, $\|A_1 - AO_1\|_F \le a_1, \|A_2 - AO_2\|_F \le a_2$, $\sigma_r(A) \ge \lambda$. Suppose $\hat{O}$ is the solution to Wahba's problem,

$$\hat{O} = \arg\min_{O\in\mathbb{O}_r} \|A_2 O - A_1\|_F ,$$

$$\text{or equivalently} \quad \hat{O} = UV^\top, \text{ if } A_2^\top A_1 = U\Sigma V^\top \text{ is the SVD.}$$

Then $\hat{O}$ satisfies

$$\left\|\hat{O} - O_2^\top O_1\right\|_F \le \frac{2(a_1+a_2)}{\lambda}. \tag{3.12}$$

The next Proposition 1 provides a sharper convergence rate when Step 2 is applied (with only complete pieces) and the random scores are sub-Gaussian distributed.

Proposition 1. Suppose $Z(t) = \mu(t) + \sum_{k\ge1} \xi_k \phi_k(t)$ is the Karhunen-Loève decomposition, where $\{\phi_k(t)\}_{k\ge1}$ is the fixed eigen-function and $\{\xi_k\}_{\ge1}$ are random scores. In addition to the assumptions of Theorem 1, we further assume the normalized leading r scores, $\tilde{\xi} = \{\xi_k/\lambda_k^{1/2}(G)\}_{k=1}^r$, is sub-Gaussian distributed such that $\mathbb{E}\exp(t\tilde{\xi}^\top u) \le \exp(C\|u\|_2^2)$ for any $u \in \mathbb{R}^r$, the tail part $Z^{(-r)}(t) = \sum_{k\ge r+1} \xi_k\phi_k(t)$ satisfies $\sup_t \mathbb{E}|Z^{(-r)}(t)|^4 \le Cr/(n^*\gamma)$, and the noise satisfies $(\mathbb{E}|\epsilon|^4)^{1/2} \le Cr/\gamma$. Then the proposed procedure with Step 2 yields the following rate of convergence,

$$\mathbb{E}\|\hat{G} - G\|_{HS} = O\left(\sqrt{r\gamma/n^*} + p^{-1}\right). \tag{3.13}$$

Here, $n^* = \min_l n_l^*$ and n_l^* is defined in (2.3).

Remark 4. We briefly compare the convergence rates of step 2 and step 2'. First, n^* when using complete sample is no greater than that of using both complete and incomplete subjects. On the other hand, the factor γ^2 in (3.11) is greater than $r\gamma$ in the counterpart of (3.13). This is because the $\hat{A}_l$ calculated via the standard sample covariance matrix as in Step 2 possesses sharper convergence rate than the one calculated via extended sample covariance matrix as in Step 2', as demonstrated by Lemma 7. Therefore, there is a trade off between using Steps 2 or 2'. Generally speaking, we recommend using Step 2' when most subjects are with noncontiguous observations (missing values); otherwise Step 2 is preferred.

4. Numerical Experiments

Simulations: In this section, we investigate the numerical performance for the proposed procedure by a series of simulation studies. For each setting, we generate $X_{ij} = \sum_{k=1}^{K} \xi_{ik}\phi_k(t_{ij}) + \epsilon_{ij}$, where $i = 1, \ldots, n$, $j = 1, \ldots, p$, and t_{ij} are equally spaced p values on $[0, 1]$. We observe a contiguous ($\delta = d/p$) portion of trajectory for each subject. All simulation results are based on 100 repetitions.

The first simulation setting is designed to assess the basic performance

of the proposed method and explore the choices of tuning parameters. Particularly, we set $p = 30$, the true rank $K = 3$ and the eigenfunctions $\{\phi_k(t)\}$ as linear combinations of $M = 10$ cubic B-splines with equally spaced knots as visualized in Figure 3. The random scores $\{\xi_{ik}\}$ are i.i.d normal with variances $(\lambda_1, \lambda_2, \lambda_3) = (4^2, 3^2, 2^2)$. The errors ϵ_{ij} are i.i.d normal with variance 1. We let the length of observation band $d = 10$, so that each observation band covers one-third (d/p) of the total domain. We further let each contiguous subset of length d be observable by $n_{rep} = \{10, 20, 50\}$ subjects, which means the total sample size $n = n_{rep} \times (p-d+1) = 210, 420, 1050$. We apply the proposed method in Section 2 with the rank r selected by cross-validation as described in Section 2, and report relative estimation errors for different choices of tuning parameters b and a in Table 1. Here, the relative estimation error in all simulation settings is defined as $\|\hat{G} - G\|_{HS}/\|G\|_{HS}$. We can see that the estimation error decreases as sample size increases, and the performance is not sensitive to the values of (b, a) as long as b is slightly smaller than bandwidth d and a is small. The cross-validation of the proposed method tends to slightly over-select r, but over-selection does not affect much the RMSE of covariance estimation in our simulation settings. In the following simulations, we always use bandwidth $b = \lceil 0.7 \cdot d \rceil$ and incremental parameter $a = \lceil 0.1 \cdot d \rceil$

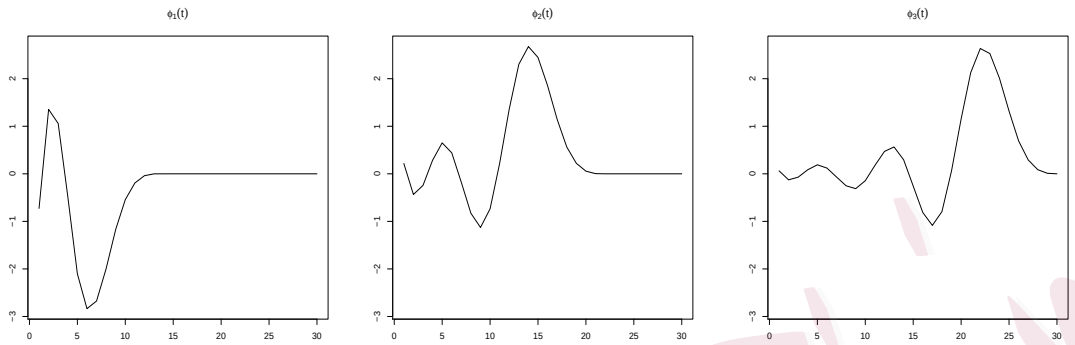

Figure 3: The first three eigenfunctions used in the simulations to generate the data.

The second simulation setting further explores the performance under different settings. Particularly, let $p = 30$ and the fraction of observable domain $\delta = \{1/5, 1/3, 1/2\}$. In addition to the previous setting with $K = 3$, we also consider another one such that $K = 10$, the score variances $(\lambda_1, \ldots, \lambda_{10}) = (4^2, 3^2, 2^2, 2^{-4}, \ldots, 2^{-10})$, ϕ_1, ϕ_2, ϕ_3 are the same as previous settings, and $\phi_k(t) = \sqrt{2}\sin(k\pi t)$ for $k = 4, \ldots, 10$ (and all 10 functions are orthonormalized). Similarly to the first simulation setting, we implement the proposed procedure with r selected by cross-validation, $b = \lceil 0.7 \cdot d \rceil$ and $a = \lceil 0.1 \cdot d \rceil$, then report the results in Table 2. We can see that the proposed procedure still performs well when there are moderate deviations to the reduced-rank structure. The estimation error decreases as the observed partial trajectory covers a larger fraction of the entire trajectory. It is

Table 1: Results for simulation 1: the average relative error over 100 simulations are shown, with the standard error in parentheses. Here a and b are different choices of tuning parameters, and the results are stable.

	$n_{rep} = 10$	$n_{rep} = 20$	$n_{rep} = 50$
$b = 7, a = 1$	0.324 (0.17)	0.224 (0.14)	0.123 (0.06)
$b = 7, a = 2$	0.325 (0.16)	0.221 (0.13)	0.132 (0.1)
$b = 8, a = 1$	0.314 (0.17)	0.23 (0.14)	0.13 (0.09)
$b = 8, a = 2$	0.364 (0.17)	0.292 (0.19)	0.126 (0.08)
$b = 9, a = 1$	0.326 (0.16)	0.227 (0.15)	0.119 (0.07)
$b = 9, a = 2$	0.347 (0.15)	0.214 (0.11)	0.145 (0.11)

worth mentioning that the selected rank r for the cases $K = 10$ increases as sample size increases, with an average value $r = 4.25$ for $d/p = 1/3$ and $n_{rep} = 50$.

The third simulation explores the performance when there are further missing values within the observable fraction of the domain. The setting is the same as in the first simulation, except that the data have 5%, 10% or 15% missing rate. The same as the previous two simulations, we implement the proposed procedure with r selected by cross-validation, $b = \lceil 0.7 \cdot d \rceil$ and $a = \lceil 0.1 \cdot d \rceil$, then report the results in Table 3. We can see that

Table 2: Results for simulation 2: the average relative error over 100 simulations are shown, with the standard error in parentheses. Here K is the total number of eigenfunctions used to generate the covariance and δ denotes the fraction of domains observed.

	$K = 3$			$K = 10$		
	$n_{rep} = 10$	$n_{rep} = 20$	$n_{rep} = 50$	$n_{rep} = 10$	$n_{rep} = 20$	$n_{rep} = 50$
$\delta = 1/5$	0.43 (0.17)	0.397 (0.2)	0.294 (0.21)	0.461 (0.16)	0.403 (0.18)	0.304 (0.19)
$\delta = 1/3$	0.341 (0.17)	0.237 (0.16)	0.135 (0.1)	0.322 (0.16)	0.248 (0.14)	0.143 (0.06)
$\delta = 1/2$	0.243 (0.11)	0.17 (0.07)	0.113 (0.05)	0.248 (0.1)	0.165 (0.05)	0.114 (0.04)

the proposed procedure performs reasonably well when there are moderate amount of missing values, and the performance improves as sample size goes large.

The fourth simulation compares the performance of the proposed method with the matrix completion method proposed in Descary and Panaretos (2018). The data generating procedure is the same as the one in previous simulations. The matrix completion method is implemented using the Matlab code downloaded from authors' website. The method requires an input of rank r, and they propose using a scree-plot to manually determine the rank (looking for an 'elbow' in the plot). Since this approach is not feasible in simulation settings, we use the true rank r in this simulation setting for

Table 3: Results for simulation 3: the average relative error over 100 simulations are shown, with the standard error in parentheses. Here "missing" is the percentage of missing values within the observed domain.

missing	$n_{rep} = 10$	$n_{rep} = 20$	$n_{rep} = 50$	$n_{rep} = 100$
5%	0.36 (0.14)	0.24 (0.12)	0.16 (0.07)	0.12 (0.06)
10%	0.39 (0.16)	0.29 (0.13)	0.19 (0.08)	0.13 (0.05)
15%	0.42 (0.13)	0.32 (0.13)	0.22 (0.1)	0.16 (0.06)

both methods. The results are reported in Table 4. The relative performance depends on the fraction of domain observed. For $\delta = 1/2$, both methods work fine, and the matrix completion method is slightly better in a small sample size ($n_{rep} = 10$). For $\delta = 1/3$, both methods work fine, the proposed method is slightly better in larger sample sizes. For $\delta = 1/5$, neither of the methods work well for a small sample size ($n_{rep} = 10$), although the error for the matrix completion method is not as large as for the proposed method. When n increases, the error of the proposed method decreases to a reasonably small level; the matrix completion method is less satisfactory in this case.

Application to midlife women's working memory study: We downloaded the data from SWAN database (link: `http://www.icpsr.umich.`

Table 4: Results for simulation 4: the average relative error over 200 simulations are shown, with the standard error in parentheses. Here "MatComp" is the matrix completion method proposed in Descary and Panaretos (2018), and δ denotes the fraction of domains observed.

		$n_{rep} = 10$	$n_{rep} = 20$	$n_{rep} = 50$	$n_{rep} = 100$
$\delta = 1/5$	proposed	0.37 (0.11)	0.27 (0.09)	0.17 (0.06)	0.12 (0.04)
	MatComp	0.32 (0.06)	0.27 (0.04)	0.23 (0.02)	0.22 (0.02)
$\delta = 1/3$	proposed	0.26 (0.10)	0.2 (0.06)	0.12 (0.04)	0.08 (0.03)
	MatComp	0.29 (0.08)	0.2 (0.05)	0.14 (0.03)	0.11 (0.02)
$\delta = 1/2$	proposed	0.26 (0.11)	0.18 (0.07)	0.12 (0.05)	0.08 (0.03)
	MatComp	0.24 (0.08)	0.17 (0.05)	0.11 (0.03)	0.08 (0.02)

edu/icpsrweb/ICPSR/series/00253). The study examines the physical, biological, psychological and social health of women during their middle years. In this section, we focus on the measurement of working memory, i.e., the ability to manipulate information held in memory. In this study, working memory was assessed by digit span backwards (DSB) (Corporation, 1997): participants repeat strings of single-digit numbers backwards, with 2 trials at each string length, increasing from 2 to 7, stopped after errors in both trials at a string length, and scored as the number of correct

trials (range, 0-12). The testing was first administered at the 4th follow-up to 2709 women, and repeated in 6th and subsequent visits. The data up to the 10th visit are publicly available. We exclude those subjects who had dropped out before the 10th follow-up visit, leaving us a sample size of $n = 2016$. Following previous literature, we did not use the first measurement to alleviate the practice effect on testing results (Karlamangla et al., 2017). Instead, we focused on the age range $\mathcal{T} = [48, 62]$. Each subject has up to five years of consecutive data, and the average number of follow-ups is 3.3. We applied the proposed method as described in Section 2 to estimate the covariance function, using a rank $r = 3$ selected by cross-validation, a band parameter $b = 4$ and an increment parameter $a = 1$. The estimated covariance surface is shown in the left panel of Figure 4. We can see that the variance is bigger at the middle part around age 55.

The nonparametric covariance estimation serves as a stepping stone for further functional data analysis. In the following, we perform functional principal component analysis for the working memory trajectories and examine how the shape of trajectories depends on education (less than high school, high school, some college/technical school, college graduate, post-graduate), controlling for race (Black, Chinese, Japanese, Caucasian/White Non-Hispanic, Hispanic) and difficulty paying for basics (no hardship, some-

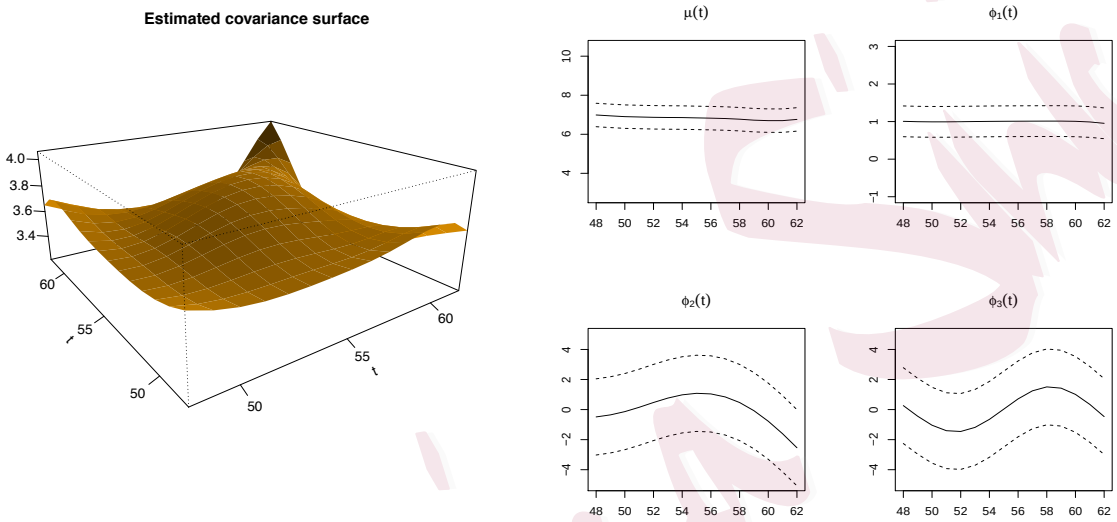

Figure 4: Left: The estimated covariance surface of the working memory data for women aged between 48 to 62. Right: The estimated mean function and the estimated eigenfunctions corresponding to the largest three modes of variation, where the dashed lines are 95% bootstrap simultaneous confidence bands.

what hard, very hard). These are just for illustration of the functional data methods, and a thorough analysis for this complex data set is beyond the scope of this paper.

Given the estimated covariance, we conducted functional principal component analysis based on Karhunen-Loève expansion $Z(t) = \mu(t)+\sum_j \xi_j\phi_j(t)$. Here $\{\phi_j(t), j \geq 1\}$ is an orthonormal basis which consists of eigenfunctions of G, and $\{\xi_j = \int(Z(t) - \mu(t))\phi_j(t)dt : j \geq 1\}$ are (random) scores. Intuitively, the first K terms expansion, $\mu(t) + \sum_{j=1}^{K} \xi_j\phi_j(t)$, forms a K-dimensional representation of $Z(t)$ with the smallest unexplained variance. The smoothed mean function and the first three estimated eigenfunctions $\{\phi_j(t), j = 1, 2, 3\}$ are visualized in the right panel of Figure 4. We also constructed 95% confidence bands for these quantities using the nonparametric bootstrap method as outlined in Hall and Hosseini-Nasab (2006). Best linear prediction methods as used in Yao et al. (2005) were applied to obtain estimates of ξ_j.

The mean function shows that working memory function for a middle-age woman is, on average, decreasing as one gets older. With longitudinal declines on average, there are individual differences in working memory aging and possible improvements in performance over multiple years. The first eigenfunction $\phi_1(t)$ is close to a horizontal line. Therefore $\phi_1(t)$ can be in-

terpreted as a size component: subjects with positive score in the direction of this eigenfunction have better working memory function than an average woman for all ages between 48-62. Regression analysis show that this component is significantly positively correlated with education level, which means that people with higher education tend to have higher working memory scores over the entire period. The other two covariates, financial status and race, are also statistically significant. The second eigenfunction $\phi_2(t)$ has a reversed U-shape with the maximum at around age = 55. This can be interpreted as a contrast of changing pattern before and after Age 55, which possibly relates to the menopausal transition, resilience and compensatory mechanisms (Fuh et al., 2006; Greendale et al., 2009; Hahn and Lachman, 2015). Subjects with positive score in the direction of this eigenfunction have an increase in working memory before Age 55 and a fast decline after Age 55. Regression analysis show that education is a significant factor, with the post graduate education group having a more prominent reversed U-shape pattern. The other two covariates are not statistically significant. The third component $\phi_3(t)$ crosses the zero line around Age 55, representing a complementary effect to the second component.

This functional data analysis perspective differs from traditional linear mixed effect models, because the modes of variation for individual chrono-

logical aging trajectories are extracted non-parametrically from the data (FPC components), and one can examine how the shape of the trajectories interacts with other covariates. In comparison, traditional linear mixed effect models (Karlamangla et al., 2017) often control these covariates as fixed main effects.

5. Discussions

In this paper, we focused on data observed on a regular equally-spaced grid; while the proposed sequential aggregating method can be readily extended to the setting where the observational times are irregular and random. Adjustments need to be made to step 2. Especially, the sample covariance estimate for Σ_l in step 2 is not applicable if data is irregularly observed. One can first adopt a bivariate local linear smoothing method (Yao et al., 2005) to estimate the covariance on the observable part (the diagonal banded area), say $\tilde{G}(s,t)$, for $|s-t| < \delta$. Then for each piece l, take the corresponding sub-piece from $\tilde{G}(s,t)$, evaluate that on a pre-defined regular grid I_l, use that as $\hat{\Sigma}_l$. All other steps remain the same.

Acknowledgment

The authors thank the editor and two anonymous referees for their helpful comments, which greatly help improve the presentation of this paper.

References

Berger, M. P. (1986). A comparison of efficiencies of longitudinal, mixed longitudinal, and cross-sectional designs. *Journal of Educational Statistics*, 11(3):171–181.

Bickel, P. J. and Levina, E. (2008). Regularized estimation of large covariance matrices. *The Annals of Statistics*, pages 199–227.

Bishop, W. E. and Byron, M. Y. (2014). Deterministic symmetric positive semidefinite matrix completion. In *Advances in Neural Information Processing Systems*, pages 2762–2770.

Cai, T. T., Ren, Z., and Zhou, H. H. (2016). Estimating structured high-dimensional covariance and precision matrices: Optimal rates and adaptive estimation. *Electronic Journal of Statistics*, 10(1):1–59.

Cai, T. T. and Yuan, M. (2012). Adaptive covariance matrix estimation through block thresholding. *The Annals of Statistics*, 40(4):2014–2042.

Cai, T. T. and Zhang, A. (2016). Minimax rate-optimal estimation of high-dimensional covariance matrices with incomplete data. *Journal of Multivariate Analysis*, 150:55–74.

Cai, T. T., Zhang, C.-H., and Zhou, H. H. (2010). Optimal rates of convergence for covariance matrix estimation. *The Annals of Statistics*, 38(4):2118–2144.

Corporation, P. (1997). Wais-iii and wms-iii: Technical manual. *San Antonio, TX: Psychological Corporation/Harcourt Brace*.

Delaigle, A. and Hall, P. (2013). Classification using censored functional data. *Journal of the American Statistical Association*, 108(504):1269–1283.

Delaigle, A. and Hall, P. (2016). Approximating fragmented functional data by segments of markov chains. *Biometrika*, 103(4):779–799.

Descary, M.-H. and Panaretos, V. M. (2018). Recovering covariance from functional fragments. *Biometrika*, 106(1):145–160.

Fan, J., Huang, T., and Li, R. (2007). Analysis of longitudinal data with semiparametric estimation of covariance function. *Journal of the American Statistical Association*, 102(478):632–641.

Fuh, J.-L., Wang, S.-J., Lee, S.-J., Lu, S.-R., and Juang, K.-D. (2006). A longitudinal study of cognition change during early menopausal transition in a rural community. *Maturitas*, 53(4):447–453.

Greendale, G., Huang, M., Wight, R., Seeman, T., Luetters, C., Avis, N., Johnston, J., and Karlamangla, A. (2009). Effects of the menopause transition and hormone use on cognitive performance in midlife women. *Neurology*, 72(21):1850–1857.

Hahn, E. A. and Lachman, M. E. (2015). Everyday experiences of memory problems and control: The adaptive role of selective optimization with compensation in the context of memory decline. *Aging, Neuropsychology, and Cognition*, 22(1):25–41.

Hall, P. and Hosseini-Nasab, M. (2006). On properties of functional principal components analysis. *Journal of the Royal Statistical Society: Series B (Statistical Methodology)*, 68(1):109–126.

Hedden, T. and Gabrieli, J. D. (2004). Insights into the ageing mind: a view from cognitive neuroscience. *Nature reviews neuroscience*, 5(2):87–96.

Helms, R. W. (1992). Intentionally incomplete longitudinal designs: I. methodology and comparison of some full span designs. *Statistics in medicine*, 11(14-15):1889–1913.

James, G. M., Hastie, T. J., and Sugar, C. A. (2000). Principal component models for sparse functional data. *Biometrika*, 87(3):587–602.

Karlamangla, A. S., Lachman, M. E., Han, W., Huang, M., and Greendale, G. A. (2017). Evidence for cognitive aging in midlife women: Study of women's health across the nation. *PloS one*, 12(1):e0169008.

Kneip, A. and Liebl, D. (2017). On the optimal reconstruction of partially observed functional data. *arXiv preprint arXiv:1710.10099*.

Kolar, M. and Xing, E. P. (2012). Consistent covariance selection from data with missing values. In *Proceedings of the 29th International Conference on Machine Learning (ICML-12)*, pages 551–558.

Li, Y. and Hsing, T. (2010). Uniform convergence rates for nonparametric regression and principal component analysis in functional/longitudinal data. *The Annals of Statistics*, 38(6):3321–3351.

Loh, P.-L. and Wainwright, M. J. (2012). High-dimensional regression with noisy and missing data: Provable guarantees with nonconvexity. *The Annals of Statistics*, 40(3):1637–1664.

Lounici, K. et al. (2014). High-dimensional covariance matrix estimation with missing observations. *Bernoulli*, 20(3):1029–1058.

Peng, J. and Paul, D. (2009). A geometric approach to maximum likelihood estimation of the functional principal components from sparse longitudinal data. *Journal of Computational and Graphical Statistics*, 18(4):995–1015.

Picard, R. R. and Cook, R. D. (1984). Cross-validation of regression models. *Journal of the American Statistical Association*, 79(387):575–583.

Press, W. H., Teukolsky, S. A., Vetterling, W. T., and Flannery, B. P. (1992). *Numerical Recipes in C (2Nd Ed.): The Art of Scientific Computing*. Cambridge University Press, New York, NY, USA.

Rice, J. A. and Silverman, B. W. (1991). Estimating the mean and covariance structure nonparametrically when the data are curves. *Journal of the Royal Statistical Society. Series B (Methodological)*, pages 233–243.

Rönnlund, M., Nyberg, L., Bäckman, L., and Nilsson, L.-G. (2005). Stability, growth, and decline in adult life span development of declarative memory: cross-sectional and longitudinal data from a population-based study. *Psychology and aging*, 20(1):3.

Wahba, G. (1965). A least squares estimate of satellite attitude. *SIAM review*, 7(3):409–409.

Xiao, L., Li, Y., and Ruppert, D. (2013). Fast bivariate p-splines: the sandwich smoother. *Journal of the Royal Statistical Society: Series B (Statistical Methodology)*, 75(3):577–599.

Yao, F., Müller, H.-G., and Wang, J.-L. (2005). Functional data analysis for sparse longitudinal data. *Journal of the American Statistical Association*, 100(470):577–590.

Department of Statistics, University of Wisconsin-Madison

Department of Biostatistics & Bioinformatics, Duke University

E-mail: anruzhang@stat.wisc.edu

Department of Statistics, University of Pittsburgh

E-mail: khchen@pitt.edu